

## Effect of high temperature AlN buffer layer thickness on the properties of $\text{Al}_x\text{Ga}_{1-x}\text{N}$ epilayers grown by HVPE

Tae-Hun Kang<sup>a</sup>, Jin-Ho Kim<sup>a</sup>, Tae-Young Lim<sup>a</sup>, Jonghee Hwang<sup>a,\*</sup>, Hae-Kon Oh<sup>b</sup>, Young-Jun Choi<sup>b</sup> and Hae-Yong Lee<sup>b</sup>

<sup>a</sup>Korea Institute of Ceramic Engineering and Technology, Seoul 153-801, Republic of Korea

<sup>b</sup>LumiGNtech Co., 233-5 Gasan-dong, Gueumcheon-gu, Seoul 153-801, Republic of Korea

$\text{Al}_x\text{Ga}_{1-x}\text{N}$  epilayers were grown on a high temperature AlN buffer grown sapphire substrate by HVPE. The nitridation and AlN buffer growth temperature was kept constant at 1110°C and buffer layer growth time was varied from 1 min to 3 min. The effects of nitridation of the sapphire substrate and buffer layer thickness on the morphological, structural and optical properties of the  $\text{Al}_x\text{Ga}_{1-x}\text{N}$  layers were investigated. The crystal quality of  $\text{Al}_x\text{Ga}_{1-x}\text{N}$  epilayers that were grown on the high temperature AlN buffer layer were better than that grown on the nitridated sapphire substrate. In addition, crystal quality improved when the buffer layer thickness changed from 162 to 205 nm, but was degraded when the buffer layer thickness was increased to 267 nm. These results indicate that an optimal AlN buffer layer thickness of approximately 200 nm is required for minimizing threading dislocations.

**Key words:** A1. Growth time, A3. HVPE, B1. AlGa<sub>N</sub>, B1. AlN, B1. Buffer.

### Introduction

Among III-nitride wide band gap semiconductors, AlN and AlGa<sub>N</sub> alloy semiconductors have recently attracted considerable attention because of their applications in high-power and high-frequency electronic devices and deep ultraviolet (UV) optoelectronic devices. To realize these devices, the epitaxial growth of high quality AlN and  $\text{Al}_x\text{Ga}_{1-x}\text{N}$  with a high aluminum (Al) content is required [1]. However, the growth of thick, crack-free  $\text{Al}_x\text{Ga}_{1-x}\text{N}$  with a high Al molar fraction is difficult due to the large lattice mismatch between  $\text{Al}_x\text{Ga}_{1-x}\text{N}$  and the sapphire substrate. There have been many reports of high quality  $\text{Al}_x\text{Ga}_{1-x}\text{N}$  epilayers grown on various types of buffer layers, such as AlN buffers [2, 3], GaN buffers, [4], superlattices [5, 6] and on patterned sapphire substrates [7]. Among these options, a GaN buffer layer is not a good choice for producing deep UV-LEDs, because they tend to absorb UV light strongly. It is difficult to fabricate a Superlattice by HVPE. On sapphire substrates, a low temperature AlN layer is typically used as a nucleation layer (NL) to avoid cracks in  $\text{Al}_x\text{Ga}_{1-x}\text{N}$  that is caused by lattice mismatch [8]. Therefore, an AlN layer represents the optimal choice for a buffer layer material for growing high quality  $\text{Al}_x\text{Ga}_{1-x}\text{N}$  epilayers by HVPE. In this study,  $\text{Al}_x\text{Ga}_{1-x}\text{N}$  epilayers were grown

on nitridation only sapphire substrates and on high temperature (HT) AlN buffer layers by HVPE and the characteristics of the produced epilayers were examined. To investigate the effects of AlN buffer layer thickness on the properties of  $\text{Al}_x\text{Ga}_{1-x}\text{N}$  epilayer, a series of AlN buffer layers were grown with different growth times at a fixed Al flux ratio. The thicknesses of the resulting AlN buffer layer were 162, 205 and 267 nm, respectively.

### Experimental

Fig. 1 shows a schematic diagram of the HVPE system used in this study. The process zone consisted of two parts, namely, the source zone and the growth zone. Ammonia ( $\text{NH}_3$ ) gas and hydrochloric acid (HCl) gas were used as the active gases, and metallic gallium and aluminum were used as group III precursors. The substrate used was 2 inch (0001) sapphire. The group III precursors were located in a separate tube at a temperature of 750°C for metallic Ga and 550°C for

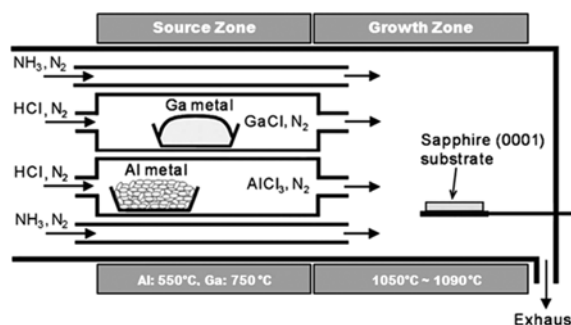
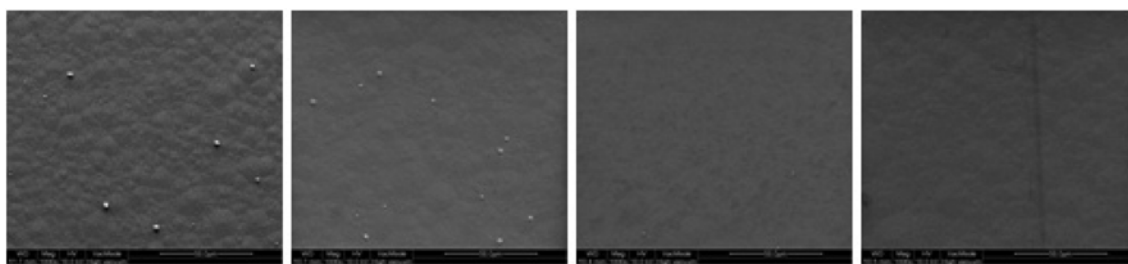


Fig. 1. Schematic diagram of the HVPE system used in this study.

\*Corresponding author:  
Tel : +82-2-3282-2428  
Fax: +82-2-3282-7814  
E-mail: jhhwang@kicet.re.kr

**Table 1.** Growth conditions of  $\text{Al}_x\text{Ga}_{1-x}\text{N}$  epilayers.

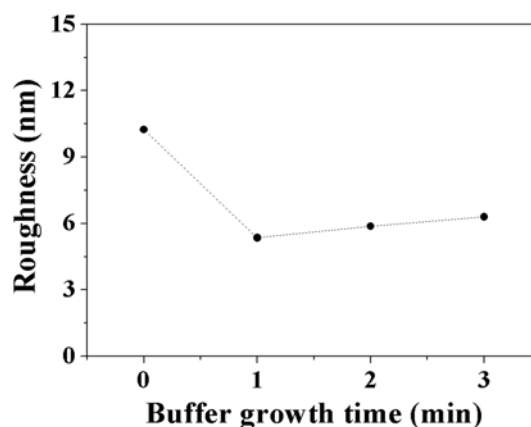
Sample	Nitridation		AlN buffer layer		AlGa <sub>x</sub> N epilayer	
	Nitridation temperature [°C]	Nitridation time [min]	Growth temperature [°C]	Growth time [min]	Growth temperature [°C]	Growth time [min]
a	1110	8	1110	0	1110	5
b	1110	8	1110	1	1110	5
c	1110	8	1110	2	1110	5
d	1110	8	1110	3	1110	5

**Fig. 2.** FE-SEM images of the  $\text{Al}_x\text{Ga}_{1-x}\text{N}$  epilayers grown on AlN buffer layer with different growth times; (a) nitridation, (b) 1 min, (c) 2 min and (d) 3 min.

metallic Al, respectively, to inhibit the generation of AlCl which degrades the quartz reactor [9]. GaCl and AlCl<sub>3</sub> gases were generated by reaction with HCl at source zone and were then transported towards the radiatively heated substrate by the N<sub>2</sub> carrier gas. After the nitridation and additional high temperature AlN buffer layer growth,  $\text{Al}_x\text{Ga}_{1-x}\text{N}$  epilayers were grown in the growth zone. Table 1 shows the growth conditions for the nitridation, AlN buffer layers and  $\text{Al}_x\text{Ga}_{1-x}\text{N}$  epilayers. The  $\text{Al}_x\text{Ga}_{1-x}\text{N}$  epilayers were grown on different AlN buffer layer thicknesses. To prepare different AlN buffer layer thicknesses, the AlN buffer layers were grown using growth times from 1 to 3 min. at intervals of 1 min with the other growth conditions maintained constant. The growth time for  $\text{Al}_x\text{Ga}_{1-x}\text{N}$  epilayers was 5 min for all samples. The grown epilayers were characterized by high-resolution scanning electron microscopy with a cathodoluminescence system (SEM-CL, MonoCL4, Gatan, USA), a surface profiler (DEKTA 150, Veeco, USA), high resolution X-ray diffraction (HR-XRD, X'pert MRD, Panalytical, Netherland), Raman spectrophotometer (NRS 3100, Jasco, Japan) and transmission electron microscopy (TEM, JEM-2000EX, JEOL, Japan).

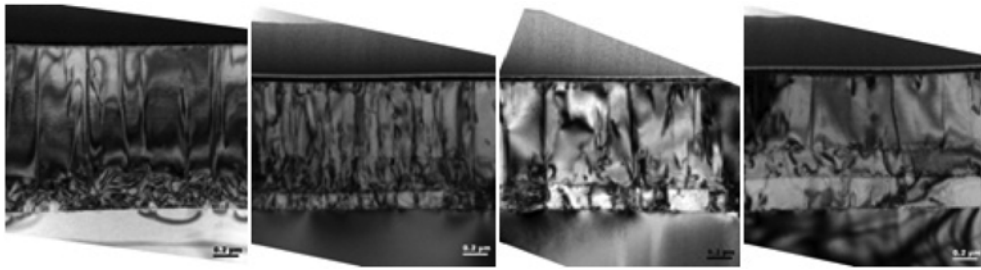
## Results and discussion

Fig. 2 shows an FE-SEM image of the  $\text{Al}_x\text{Ga}_{1-x}\text{N}$  layer grown on a nitridated sapphire substrate and on different thicknesses of AlN buffer layers. The images of the entire  $\text{Al}_x\text{Ga}_{1-x}\text{N}$  epilayers surface showed mirror-like surfaces. However, micro-cracks were observed in samples (a) and (b). In the case of the AlN buffer layer, when the thickness was increased, the number of micro-cracks was decreased and no micro-

**Fig. 3.** Surface roughness of the  $\text{Al}_x\text{Ga}_{1-x}\text{N}$  epilayers grown on an AlN buffer layer with different growth times; (a) nitridation, (b) 1 min, (c) 2 min and (d) 3 min.

cracks were detected in sample (c) and (d).

Fig. 3 shows the surface roughness (RMS) results for the  $\text{Al}_x\text{Ga}_{1-x}\text{N}$  epilayers grown on nitridated sapphire substrate and different thicknesses of AlN buffer layers. The surface roughness of the  $\text{Al}_x\text{Ga}_{1-x}\text{N}$  epilayers were 10.24, 5.35, 5.87 and 6.30 nm, respectively. The surface roughness was clearly improved in the case of an AlN buffer layer, but the effect of the thickness of the buffer layer was insignificant. The rough surface of  $\text{Al}_x\text{Ga}_{1-x}\text{N}$  epilayers grown on nitridated sapphire substrates might be caused by the roughness of the actual nitridated sapphire substrate used. The surface of the nitridated sapphire substrate showed many protrusions when it was nitridated at high temperature [10]. Another reason for the smooth surface of the  $\text{Al}_x\text{Ga}_{1-x}\text{N}$  epilayers grown on AlN buffer layer might be the tendency for two-dimensional (2D) growth by the low



**Fig. 4.** Cross-sectional TEM images of the  $\text{Al}_x\text{Ga}_{1-x}\text{N}$  epilayers grown on an AlN buffer layer with different growth times; (a) nitridation, (b) 1 min, (c) 2 min and (d) 3 min.

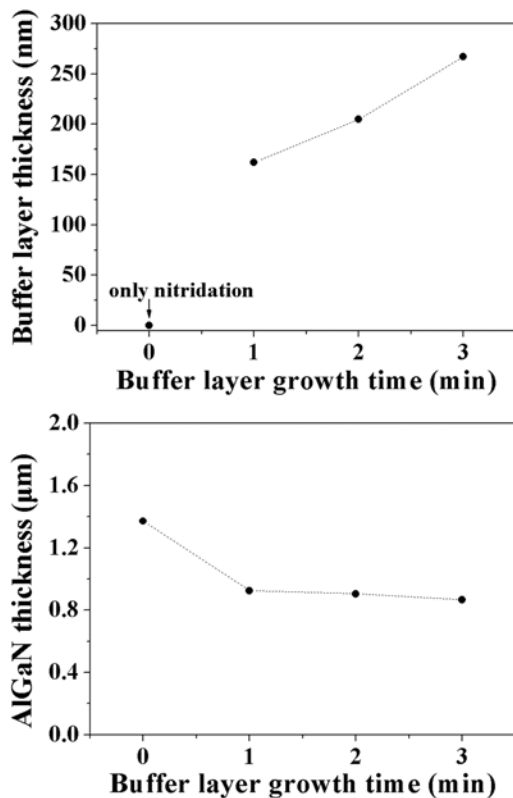
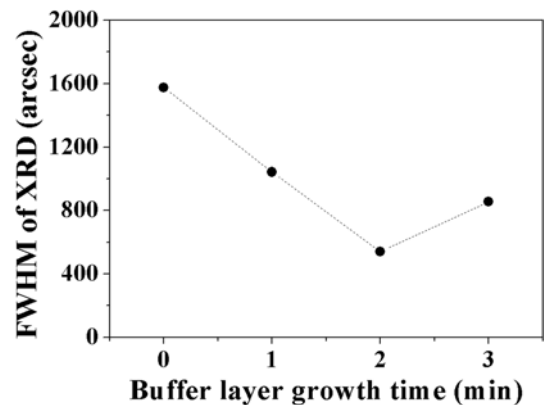


**Fig. 5.** The thickness variation of (a) AlN buffer layers, (b)  $\text{Al}_x\text{Ga}_{1-x}\text{N}$  epilayers.

value of the lattice mismatch [11].

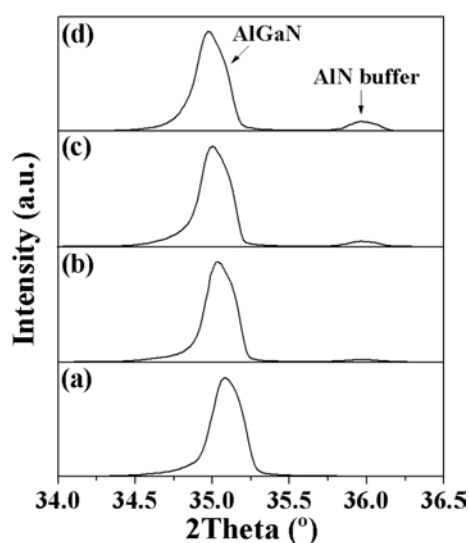
Fig. 4 shows cross-sectional TEM images of the  $\text{Al}_x\text{Ga}_{1-x}\text{N}$  epilayers grown on sapphire substrates with nitridation and various thicknesses of AlN buffer layers. The  $\text{Al}_x\text{Ga}_{1-x}\text{N}$  epilayer grown on the nitridated sapphire substrate showed a high density of threading dislocation (TD) and the TD density of the  $\text{Al}_x\text{Ga}_{1-x}\text{N}$  epilayers decreased with the help of the AlN buffer layer. The TD density of the  $\text{Al}_x\text{Ga}_{1-x}\text{N}$  epilayers decreased with increasing growth time of the AlN buffer layer up to 2 min and then increased again with a growth time of 3 min for sample (d). Therefore, the thickness of the AlN buffer layer appears to be a key factor that can strongly affect the structural properties of the  $\text{Al}_x\text{Ga}_{1-x}\text{N}$  epilayer [12].

Fig. 5 shows the thickness of the AlN buffer layers and  $\text{Al}_x\text{Ga}_{1-x}\text{N}$  epilayers, as determined by cross-



**Fig. 6.** The relationship between buffer growth time and FWHM of XRD  $\omega$ -scan rocking curve of  $\text{Al}_x\text{Ga}_{1-x}\text{N}$  epilayers.

sectional TEM images in Fig. 4. The thickness of the AlN buffer layers was increased for growth times from 1 to 3 min, as shown in Fig. 5 (a). The thicknesses of the AlN buffer layers were 162, 205 and 267 nm, respectively. However, it was not possible to determine the thickness of nitridation layer of the sapphire substrate from cross-sectional TEM images. In addition, the thickness of the  $\text{Al}_x\text{Ga}_{1-x}\text{N}$  epilayer grown on nitridated sapphire substrate was 1.4  $\mu\text{m}$  and the values for the  $\text{Al}_x\text{Ga}_{1-x}\text{N}$  epilayers grown on AlN buffer layers were about 0.9  $\mu\text{m}$ . The thickness of the  $\text{Al}_x\text{Ga}_{1-x}\text{N}$  epilayer grown on the nitridated sapphire substrate was thicker than those grown on AlN buffer layers, even when the same growth time of 5 min was used, as shown in Fig. 5 (b). However, the thickness of the  $\text{Al}_x\text{Ga}_{1-x}\text{N}$  epilayers grown on AlN buffer layers of different thicknesses did not show any typical trend. The difference in the growth rate of the  $\text{Al}_x\text{Ga}_{1-x}\text{N}$  epilayers between grown on nitridated sapphire substrate and AlN buffer layer seems can be attributed to interface structure or characteristics. As shown the cross-sectional TEM images in Fig. 4, the growth mode of  $\text{Al}_x\text{Ga}_{1-x}\text{N}$  epilayer grown on nitridated sapphire substrate was very different from that for samples grown on AlN buffer layers. The high growth rate of the  $\text{Al}_x\text{Ga}_{1-x}\text{N}$  epilayer grown on nitridated sapphire substrate can be attributed to the high growth rate of initial stage of 3D growth by the rough surface characteristics of nitridated sapphire substrate [10] or



**Fig. 7.** High resolution X-ray diffraction spectra of the Al<sub>x</sub>Ga<sub>1-x</sub>N epilayers grown on AlN buffer layer with different growth times; (a) nitridation, (b) 1 min, (c) 2 min and (d) 3 min.

by damaged areas on the sapphire substrate surface [13].

Fig. 6 shows the full-width at half-maximum (FWHM)  $\omega$ -scan X-ray rocking curves from the (0002) diffraction of Al<sub>x</sub>Ga<sub>1-x</sub>N epilayers as a function of nitridation and growth time of the buffer layer. The FWHM of the XRD rocking curve is typically used to quantify the extent of relative crystalline imperfections. The rocking curves of the (0002) symmetric plane are normally responsive to screw type and mixed type threading dislocations [14]. The FWHM value for the Al<sub>x</sub>Ga<sub>1-x</sub>N epilayer grown on nitridated sapphire substrate was larger than that for the sample grown on AlN buffer layers. In addition, the FWHM value of the Al<sub>x</sub>Ga<sub>1-x</sub>N epilayers was affected by the thickness of AlN buffer layer. The FWHM values of the (0002) symmetry plane were remarkably decreased with increasing thickness of the AlN buffer layer up to 205 nm and then increased again in sample (d) where the AlN buffer layer thickness was 267 nm. This indicates that the excess thickness of the buffer layer reduced the crystallinity, although cracks were not generated. Such changes in crystallinity are consistent with the variation in the TD density shown in Fig. 4. The increase in the TD density for an AlN buffer layer thickness greater than the optimal thickness caused cracks and a reduction in the Al<sub>x</sub>Ga<sub>1-x</sub>N epilayer resulted in an improved crystalline quality.

Fig. 7 shows  $\theta$ -2 $\theta$  XRD profiles of Al<sub>x</sub>Ga<sub>1-x</sub>N epilayers. The (0002) peak position of Al<sub>x</sub>Ga<sub>1-x</sub>N epilayer grown on the nitridated sapphire substrate was 35.1°, but the values for the Al<sub>x</sub>Ga<sub>1-x</sub>N epilayers grown on the AlN buffer layer were 35.0° irrespective of the thickness of the AlN buffer layer. The peak positions were shifted to a lower value, as the buffer layer was introduced. In addition, an AlN peak also found for samples with AlN

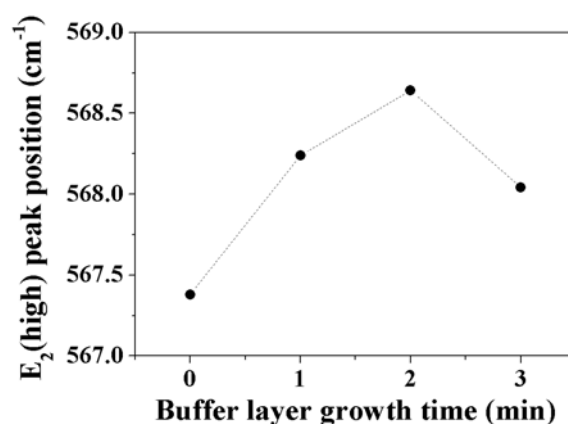


**Fig. 8.** Dependence of the Raman E<sub>2</sub> (high) peak positions of the Al<sub>x</sub>Ga<sub>1-x</sub>N epilayers grown on AlN buffer layer with different growth times.

buffer layers and their intensity increased with the thickness of the buffer layer. The Al molar fraction of the Al<sub>x</sub>Ga<sub>1-x</sub>N epilayer was determined with Vegard's law, by calculating the difference in the peak position between Al<sub>x</sub>Ga<sub>1-x</sub>N and GaN peak assuming that the (0002) peak of GaN is constant at  $2\theta = 34.53^\circ$  [11]. The calculated Al molar fractions were 0.25 and 0.30, respectively. The compositional difference might be caused by the difference in activation energy for adatom migration. Surface adatom migration of Al might be increased on the AlN buffer layer surface [10].

Fig. 8 shows the Raman E<sub>2</sub> (high) peak positions of the Al<sub>x</sub>Ga<sub>1-x</sub>N epilayers. According to Cros et al., the E<sub>2</sub> (high) peak position of Al<sub>x</sub>Ga<sub>1-x</sub>N epilayers followed the equation of  $E_2(\text{high}) = 556.3 + 51.0x$  (cm<sup>-1</sup>) within the compositional range studied ( $0.15 < x < 0.80$ ) [15]. The Al molar fractions, as determined using Vegard's law, were 0.25 and 0.30, as shown in Fig. 7. So the calculated E<sub>2</sub> (high) peak position for Al<sub>x</sub>Ga<sub>1-x</sub>N epilayers grown on nitridated sapphire substrates and AlN buffer layers were 571.09 cm<sup>-1</sup> and 569.52 cm<sup>-1</sup>. However, the measured E<sub>2</sub> (high) peak positions of the Al<sub>x</sub>Ga<sub>1-x</sub>N epilayers grown on the nitridated sapphire substrate and AlN buffer layers were 567.38, 568.24, 568.64 and 568.04 cm<sup>-1</sup>, respectively. The resulting Raman shift values for these samples were -3.71, -1.28, -0.88 and -1.48 cm<sup>-1</sup>. All the phonon modes were blue shifted with respect to the calculated value, suggesting that the Al<sub>x</sub>Ga<sub>1-x</sub>N layer is under compressive stress even though some micro-cracks were present in sample (a) and (b) [16]. Stress was decreased with increasing buffer layer thickness in the range from 162 to 205 nm but then increased again at an AlN buffer layer thickness of 267 nm for sample (d). The buffer layer thickness of 205 nm showed the effect of stress relaxation in epilayer growth. The results of TD density from TEM images, X-ray rocking curves and Raman peak position, suggest that the optimal thickness of the AlN buffer layer on the sapphire substrate is approximately 200 nm.

## Conclusions

The effect of buffer layer thickness on the qualities of  $\text{Al}_x\text{Ga}_{1-x}\text{N}$  epilayers was investigated. The buffer growth time was varied from 1 min to 3 min at intervals of 1 min. The thickness of the produced AlN buffer layers were 162, 205, 267 nm, respectively. The corresponding Al molar fractions of  $\text{Al}_x\text{Ga}_{1-x}\text{N}$  epilayers grown on nitridated sapphire substrate and AlN buffer layers were 0.26 and 0.30 each. From cross-sectional TEM images and FWHM of the XRD peak, crystal quality was clearly improved when the AlN buffer layer thickness changed from 162 to 205 nm, but then became degraded again when the buffer layer thickness was increased to 267 nm. Therefore, the AlN buffer layer thickness seems to be a key factor that can strongly affect the structural properties of the  $\text{Al}_x\text{Ga}_{1-x}\text{N}$  epilayers. Such a change in the crystal quality was consistent with the variation in Raman  $E_2$  (high) peak shift, suggesting that the optimal thickness of the AlN buffer layer on the sapphire substrate was approximately 200 nm.

## Acknowledgements

This work was financially supported by the Fundamental R&D Program for Core Technology of Materials funded by the Ministry of Knowledge Economy, Republic of Korea.

## References

1. H.J. Kim, S. Choi, D.W. Yoo, J.H. Ryou and R.D. Dupuis, *J. Crystal Growth* 310 (2008) 4880-4884.
2. Y. Jianchang, W. Junxi, L. Naixin, L. Zhe, R. Jun, and L. Jinmin, *J. Semiconductors* 30 (2009) 103001.
3. D.G. Zhao, J.J. Zhu, Z.S. Liu, S.M. Zhang and H. Yang, *Appl. Phys. Lett.* 85 (2004) 1499-1501.
4. J. Selvaraj, S.L. Selvaraj and T. Egawa, *Jpn. J. Appl. Phys.* 48 (2009) 121002.
5. M.Z. Peng, L.W. Guo, J. Zhang, X.L. Zhu, N.S. Yu, J.F. Yan, H.H. Liu, H.Q. Jia, H. Chen and J.M. Zhou, *J. Crystal Growth* 310 (2008) 1088-1092.
6. K. Pakula, J. Borysiuk, R. Bozek and J.M. Baranowski, *J. Crystal Growth* 296 (2006) 191-196.
7. N. Kuwano, Y. Kugiyama, Y. Nishikouri, T. Sato and A. Usui, *J. Crystal Growth* 311 (2009) 3085-3088.
8. X.Q. Shen, T. Ide, S.H. Cho, M. Shimizu, S. Hara, H. Okumura, S. Sonoda and S. Shimizu, *J. Crystal Growth* 218 (2000) 155-160.
9. Y. Kumagai, T. Yamane, T. Miyaji, H. Murakami, Y. Kangawa and A. Koukitu, *Phys. Stat. Sol. (c)* 0 (2003) 2498-2501.
10. J.S. Paek, K.K. Kim, J.M. Lee, D.J. Kim, M.S. Yi, D.Y. Noh, H.G. Kim and S.J. Park, *J. Crystal Growth* 200 (1999) 55-62.
11. I.S. Seo, S.J. Lee, S.H. Jang, J.M. Yeon, J.Y. Leem, Y.J. Park and C.R. Lee, *J. Crystal Growth* 241 (2002) 297-303.
12. J.O. Kim, S.K. Hong, H. Kim, K.W. Moon, C.J. Choi and K.Y. Lim, *J. Korean Phys. Soc.* 58 (2011) 1374-1379.
13. P. Ruterana, J.C. Gerard Nouet, B. Lei, H. Ye, G. Yu, M. Qi and A. Li, *Phys. Stat. Sol. (b)* 241 (2004) 2689-2692.
14. B. Heying, X.H. Wu, S. Keller, Y. Li, D. Kapolnek, B.P. Keller, S.P. DenBaars and J.S. Speck, *Appl. Phys. Lett.* 68 (1996) 643-645.
15. A. Cros, H. Angerer, O. Ambacher, M. Stutzmann, R. Hopler, T. Metzger, *Solid State Commun.* 104 (1997) 35-39.
16. F.C. Wang, C.L. Cheng, Y.F. Chen, C.F. Huang and C.C. Yang, *Semicond. Sci. Technol.* 22 (2007) 896-899.